Modeling the effects of the Wnt and mTOR signaling pathways on ASD-impacted visual processing using neural networks to reflect population dynamics

Rithvik Marri[1], John Amodeo[2]

1. American Heritage School Broward
2. Duke University

Keywords: ASD, neural network, Wnt pathway, mTOR pathway, long-range signaling

Abstract

Autism spectrum disorder (ASD) is a highly heterogeneous disorder, but two pathways, Wnt and mTOR, have been identified as significantly high-risk. The Wnt pathways produce Wnt proteins that stabilize synapses, and mTOR activates CCL5, which stimulates glutamate release. These two proteins in excess cause unnecessary synapses to form and survive, a key hallmark of ASD. We aimed to create a neural network model that uses visual processing as a base to examine the effects of the two proteins at ASD levels. We found that the perturbed networks failed to classify images as accurately as the control. This type of model can be used in future research to study population dynamics and signaling molecules in neurological disorders.

Introduction

Autism spectrum disorder (ASD) is a heterogeneous neurodevelopmental disorder with symptoms related to social interaction, communication, and hypersensitivity[1]. Vision, particularly, is one of the main senses impacted by patients with ASD[2]. The prevalence is increasing, and it is one of the more common childhood development disorders today[3]. ASD has a complex genetic etiology with hundreds of genes that are implicated in the pathology, but there are two

pathways, the Wnt pathway and the mTOR (mechanistic target of rapamycin) pathway, that are found to be increasingly high risk for the disorder. More specifically, the increase of Wnt proteins and the mTOR-activated release of CCL5 (chemokine ligand 5) protein are found in patients with ASD[4,5]. Both of these proteins have been studied in isolation and at the cell-to-cell level. However, the crosstalk between the two proteins and their involved pathways lacks research. Additionally, current research does not include the potential study of these pathways in terms of population dynamics. Because much of the brain is interconnected and constantly communicating, considering long-range signaling for the pathways could be crucial to improving understanding.

For this study, we aim to model the effects of the increased concentrations of both the Wnt and CCL5 proteins in visual processing by leveraging a neural network to capture neuronal communication. Using computational techniques allows for a more accessible form of study that still reflects human biology. By creating, testing, and analyzing this model, we aim to understand the impact of these specific proteins on ASD at the neuronal level as well as set up potential avenues for future research.

Literature Review

To study the role of CCL5 and Wnt proteins on the molecular signaling level of ASD with respect to the visual pathway, it is important to consider aspects of signal transduction. Namely, the diffusion of the signaling molecule, the receptor binding, the intracellular cascade, and finally the neuronal activity in response are events that require further explanation. Understanding how ASD pathology affects these functions is crucial to modeling how these networks are dysfunctional in patients with ASD. Both signaling pathways, WNT and mTOR, have roles in synaptic function and neuroplasticity, roles that are changed in the circuitry of patients with ASD[4,5]. The impact of altered levels of Wnt proteins and CCL5 on plasticity through synaptic

stability and release probability, respectively, is necessary to show the effects in the model and the result on visual processing.

mTOR-activated CCL5

CCL5 is a C-C chemokine, a class of small proteins present throughout the body and the brain that is potentially involved with neurotransmission and modulation[6]. It is usually implicated in cell migration and intercellular communication, along with central neuroinflammation[7]. CCL5 binds to C-C chemokine receptors, G-protein coupled receptors that are located on microglia, astrocytes, and even neurons, which were previously thought to not have these receptors. CCL5 mainly acts as a ligand for the CCR1, CCR3, and CCR5 subtypes[7]. The expression of CCL5 is regionalized within the CNS and is highest in white matter concentrated in glia and myelinated axons. But it is also present in the cerebral cortex and hippocampus, even without inflammation[8].

In relation to ASD, CCL5 has been shown to have a statistically significant relationship with hyperactivity and other symptoms of ASD[1]. The abnormal mTOR pathway in ASD can increase CCL5 production[9]. This is done because mTOR phosphorylation is elevated in the biology of patients with ASD. The mTOR activation then down-regulates the phosphorylation of glycogen synthase kinase-3 beta (GSK-3β), which proceeds to reduce the phosphorylation of cAMP response element-binding protein (CREB). Because of this process, less CREB is available to bind with CREB-binding protein (CREBBP) within the nucleus, which opens up the nuclear factor kappa-light-chain-enhancer of activated B cells (NF-κB) to bind to CREBBP instead. NF-κB binding with CREBBP results in the overexpression of CCL5[10].

After being released, CCL5 reaches neurons through volume diffusion and modulates neuronal activity through paracrine signaling, which is mediated by the expression of CCRs in neurons.

Diffusion can only happen when the extracellular concentration of CCL5 is high enough to ensure crossing across synaptic space. Once CCL5 binds to a CCR subtype, usually PTx-sensitive GCPRs, it induces a change in G proteins. The G proteins then lead to phospholipase C (PLC) translocation, hydrolysis of phosphoinositides, and inositol triphosphate (IP_3)/diacylglycerol (DAG) production. This cascade then causes the mobilization of Ca^{2+} ions, eventually activating protein kinase C (PKC). PKC then begins phosphorylation processes that increase glutamate vesicle exocytosis into the synaptic cleft[11]. Increased glutamate results in excitotoxicity, or the toxicity that arises from excitatory molecules, which can then have various negative effects on forming connections, an aspect of ASD that is discussed further.

Wnt proteins from the WNT signaling pathway

Mutations in several WNT ligands, including WNT1, WNT2, WNT3, and WNT9B, have been connected with ASD. A WNT1 missense variant present in ASD etiology can activate WNT/β-catenin signaling, and elevated levels of WNT expression have been documented in patients with ASD. This evidence suggests that the overactivation of the WNT signaling pathway is a factor in ASD pathogenesis[5]. The hyperactivation of WNT signaling can lead to neurodevelopmental defects with neuron migration, cell fate specification, and dendrite and synapse formation or function[12]. The combination of perturbed pathways along with the WNT pathway can give rise to emergent symptoms and behaviors associated with ASD[13]. It is important to understand the function and transduction of Wnt proteins within this pathway before applying it to a visual processing model.

Wnt proteins are glycoproteins that act both short- and long-range. They bind to multiple receptors, including Ror and Ryk tyrosine kinases, but mainly bind to Frizzled (Fz) receptors. This binding results in the activation of protein kinase A (PKA) and an increase in extrasynaptic AMPA receptors (AMPARs) through the phosphorylation of the GluA1 subunit of AMPARs at

serine 845. Wnt then plays a role in the migration of the extrasynaptic AMPARs by lateral diffusion. The Fz binding also activates calcium/calmodulin-dependent protein kinase II (CaMKII), which phosphorylates synaptic Ras GTPase-activating protein (SynGAP) and activates Ras-ERK signaling. These processes, along with the influx of Ca^{2+} ions, trigger actin cytoskeleton reorganization to regulate the growth of dendritic spines and the level of AMPARs[14,15].

Presynaptic development is also affected by Wnt signaling. Wnts increase synapsin 1 levels, a protein involved with the creation and function of synaptic vesicles and the induction of growth cone expansion. Wnts are also involved with axonal spreading and the growth of cone size, done through loops of microtubules at the cone[16,17]. Interestingly, the gene SYN2, coding for the protein synapsin 2, is upregulated with enhanced WNT signaling and impairs learning and memory, similar to ASD-like behaviors[15]. A different function of Wnts at the synapse has been demonstrated, involving the increase in functional $GABA_A$ receptors (GABAA-Rs), which are highly recycled and positively correlated to synaptic strength[18].

Neurotransmitter release and synaptic stability in regard to neuroplasticity

ASD is heavily implicated in abnormalities in plasticity[19], which is crucial to the control of the connections made in the CNS and specifically in the visual processing pathway. It is then important to understand how the dysfunctional mTOR and WNT signaling pathways present in ASD can have detrimental effects on neuroplasticity. Specifically, the signaling molecules of CCL5 and Wnt proteins have an effect on this process, and identifying their roles is important for building a model.

As discussed earlier in this section, the elevated levels of CCL5 due to the abnormal mTOR pathway can lead to an increase in excitatory neurotransmitter glutamate. This causes

excitotoxicity and the overexcitation of ionotropic glutamatergic receptors like NMDA and AMPA receptors. The resulting increase in calcium ion concentration in the cytosol activates the inducible isoform of NO synthase, increasing nitric oxide concentration and phosphorylating PKC and phospholipase A2. These events proceed to the enhancement of lipid peroxidation, and free radicals inhibit oxidative phosphorylation, triggering an apoptosis cascade. The ATP products, like 4-hydroxynonenal (4-HNE), may then interact with synaptic proteins and disturb the transport of glucose and glutamate, making the neurons more sensitive to excitotoxicity. The corresponding imbalance of excitation and inhibition causes new properties to appear in a neural network[20].

Wnt proteins also play a role in synaptic plasticity. Wg, part of the Wnt family of proteins, has been released from presynaptic boutons when activity is stimulated, as well as eliciting changes in synaptic functions and dynamics[21]. This evidence suggests a role for Wnt in activity-mediated plasticity. The role in question was supported with more evidence, as mossy fiber axon terminals developed in an enriched environment were similar to Wnt-induced mossy fiber granules at cerebellar synapses[22]. More specifically, Wnt has also been found to be involved with long-term potentiation (LTP), a well-studied process of plasticity. This is evidenced by the reintroduction of Wnt, initially withheld from hippocampal neurons, rapidly increasing dendritic spine growth, AMAPAR recruitment, and synaptic strength, like in the early stages of LTP[23].

Considering all of the information reviewed so far, it allows for the informed construction and modification of a visual processing model that can be influenced to reflect the changes present in ASD.

Methods

To effectively represent the pathways and the corresponding connections made in the brain, the chosen method is to create and test an artificial neural network that receives visual input in the form of image classes and assigns the most probabilistic class a set of images belongs to. The model has to be able to be adjusted for the increased levels of CCL5 and Wnt proteins that are found in patients with ASD to understand the effect these two pathways can have on visual processing.

Overview

The model is built in the Python coding language (version 3.11) and coded with the PyCharm integrated development environment. The initial input for the model is a set of images separated by the categories of dogs, cats, cars, and trucks. In the categories, there is a training subset through which the neural network works, and then a testing subset where the accuracy of the neural network is measured. Specifically, in the training phase, the neural network is given both the image and the label (the category the image is in) and trains to reduce the loss between the predicted label and the actual label. The training sessions and the loss for each session are printed and graphed. Then, in the testing phase, the neural network is given only the image and asked to predict the label, with the accuracy of these predictions represented as a percentage output.

This neural network is coded to run similarly to how human visual processing is done. It attempts to model the connections made in a human brain that are involved with vision and its aspects. As identified earlier, in an ASD brain, there are elevated levels of both CCL5 and Wnt proteins that influence both synapses and neurotransmitter release. CCL5 influences the release of glutamate, an excitatory neurotransmitter that is crucial to memory and neuroplasticity. Wnt proteins have a positive effect on synaptic stability and allow for more synapses to stay active. However, in typical development, the number of synapses is pruned

back naturally. In ASD brains, there is a surplus of synapses due to the failure of pruning mechanisms[24]. To reflect this difference in the brains of patients with ASD, the fold changes for CCL5 and Wnt are independent variables that can be adjusted in the model and have a corresponding effect on the underlying neural network nodes, layers, and connections.

Visual Input

For the computer to actually process the images that are being fed through the network, each image is converted into a form that contains usable data. The image is converted to a matrix of numbers based on pixel light intensity and RGB (red, green, and blue) values. The conversion is done with a function from the OpenCV library that was installed as a package and imported into the code. The matrix is then converted from RGB values to grayscale and resized through similar functions. Once resized, the matrix entries are converted to percentages of 255 so they can be accurately compared and then flattened down to a 2500x1 matrix. Each matrix is encoded with its label from the image classes in a dictionary that allows the label to be called back from the class itself. This will later be used in the training and testing phases of the neural network.

Neural Network

The first action the code takes for the model is to initialize the components of the neural network: the layer sizes, weights, and biases. The weights and biases are randomly generated and then modified in the training phase to become more accurate. The initialization takes a few parameters from the user to set up the network: the class list, image vector size, and hidden layer number. The image vector size determines the number of nodes in the input layer. Each

node holds something unique about the image and passes it on to subsequent nodes. The next layer in the network, one of the hidden layers, has the same number of nodes as the previous layer and receives one-to-one connections from the previous layer. This would mean that any one pixel in the image is primarily represented by one node in a layer. The values are scaled by the distinct weight matrices before moving on to the next layer. The number of hidden layers is defaulted to 4, and both the hidden layer number and the image vector size can be changed to test different cases and variables. The signals between these layers are then sequestered into a final layer. The final layer, or output layer, has a size determined by the class list. The class list itself is a list of the image labels, which are also the names of the folders containing the images for training and testing. There are four total classes, so using all of them in the class list would result in an output layer with four nodes and the corresponding data. This data is in the form of probabilities of the image being in one of the classes, with the highest probability taken to be the predicted class. In this idealized neural network, the input layer and all the hidden layers do not transfer redundant information due to the one-to-one connections. This is reminiscent of biological neural networks evolving to eliminate redundancy to become more efficient.

However, the presence of excess Wnt proteins facilitates the formation of more synapses than typical Wnt concentrations. In this model, the increased Wnt concentration in ASD is accounted for by the variable ΔWnt, or the fold change in the Wnt concentration of a patient with ASD compared to a typically developing child. For example, a ΔWnt value of 0.5 would mean a 1.5-times greater increase in Wnt concentration than the norm. This means a ΔWnt of 0 is the default. The value of ΔWnt is then used to scale up or down the downstream layer by multiplying the upstream layer by the value to find how many nodes are added or removed. This process creates redundancy because there are now nodes receiving input from more than one previous node. There would be multiple nodes in a layer that primarily represent any one pixel in the image. More connections in this modified network are similar to those in ASD patients, who

have more synapses than necessary. The identified fold change of Wnt proteins in ASD was determined in previous studies by isolating the expression of high-risk genes and found to be 1.41859 times the normal concentration[25].

Once the feedforward portion of the model is complete, there is a feedback component that updates weights and biases based on the error found in the predicted class. The encoded image label is subtracted from the output layer to get a difference matrix that is then propagated backwards through the network. This difference matrix is multiplied by the transposition of the weight matrix between the final hidden layer and the output layer and scaled by a number found by [activity of the last hidden layer * (1-the activity of the last hidden layer)] to get another difference matrix. The process is then repeated through all the hidden layers. Each difference, or delta, matrix is made into one long vector that then has its individual values squared, summed, and square-rooted to produce a single value called the Euclidean norm. If this norm is too large, it's clipped by a preset max gradient norm value that keeps the delta values small enough for backpropagation.

The layer deltas update the weights in each layer by multiplying the delta by the transposition of the layer activity. The values in the resulting matrix are multiplied by an already inputted learning rate, defaulted to 0.1, and subtracted from the existing layer weight matrix. Updating the biases is done in a similar way, with the scaled delta matrix being subtracted from the existing biases matrix instead. The cross-entropy loss of the output layer compared to the encoded image label is calculated by taking the natural log of the node values, multiplying by the encoded image label to zero out incorrect values at the wrong image class, and converting it to a positive value. This value is then returned as a loss by the model.

Training and Testing

Once the initialization, feedforward, and feedback components are defined, the model can then be trained and tested with the images in the different image classes. The training phase is where the neural network learns to classify images according to the specific class labels with which they are paired. Training takes a session count and repeats the neural network over the specified number of sessions. It uses the images specifically built in for training, feeds them through the feedforward part of the neural network, and returns a list of layer activities. Once this process occurs, the layer activities and encoded label images are passed through the feedback operation, returning the loss for each image. The mean loss is found for the whole session and then plotted to show the change in loss over the session count.

Once training is complete, the neural network is tested on a different set of images that are still separated into the various classes. These images are passed through the feedforward function of the network, and the output layer activity list is received. The output layer matrix is converted to a matrix of equal size, where all cells in the matrix are the index value of the node with the highest image class probability. The converted matrix is compared with a version of the encoded image label that is also converted to a matrix of equal size that has each cell contain the index value of the node as 1. If the two matrices match, the trial is a success, and 1 is added to the correct trial count. After testing runs through all the images, it returns a percent accuracy out of all trials and prints the value.

Network Tuning

Several functions are also at play within the neural network to represent the effect of the CCL5 concentration increase as well as create comparable data values at the nodes in each layer. The dimensions of the weight matrix are used to create a matrix of random values, defined as release maps, with the same dimensions. Importantly, these random values are selected from a

Poisson distribution centered on a value given as ΔCCL5. Similar to the ΔWnt value, which was the fold change of Wnt concentration in patients with ASD compared to typically developing children, ΔCCL5 is the fold change of CCL5 concentration. This value has been measured in several clinical trials and found to be 1.40467 times the normal concentration[3,26]. So the ASD value of ΔCCL5 would be equal to 0.40467. Poisson distributions have been found to simulate the stochastic release of neurotransmitters at synapses, and increased CCL5 concentration also results in increased excitatory neurotransmitter release, so centering the Poisson distribution at the new value of CCL5 would best replicate the effect on neurotransmitter release. The new release maps can then be multiplied by the existing weight matrices to scale the numbers and connections made between nodes similar to biological connections.

A sigmoid function is also applied to the layers in the network. The function is defined below.

$$sigmoid(x) = \frac{1}{1 + e^{-x}}$$

This function uses a node value as the negative exponent of Euler's number, adds 1 to that new value, and then divides this whole result out of 1 to make each node between 0 and 1 and maintain their relative differences. This is important to compare the output of the network to the encoded image label. Once the output layer is produced, a softmax function is applied to the layer. First, the largest node value is found and then subtracted from each node. These following negative values are used as the negative exponents of Euler's number and then divided by the sum of all the values to determine the percentage of which each one contributes to the sum. The softmax function is done like this:

$$softmax(x_i) = \frac{e^{x_i}}{\sum_{j=1}^{n} e^{x_j}}$$

The updated layer is returned and now predominantly contains node values between 0 and 1. Whichever node value is the highest is treated as the predicted image class, which is then used for training and testing.

Data Analysis

Once the training sessions are complete, the loss for each session is returned and printed. These values are also taken as a mean of all the images and plotted in a graph, with the x-axis being the session number and the y-axis being the mean loss. These values are also returned in spreadsheet form for better analysis. There will be four main model runs: the control with both ΔWnt and ΔCCL5 values being 0 indicating normal concentration, ΔWnt being at ASD levels and ΔCCL5 at 0, ΔWnt at 0 and ΔCCL5 at ASD levels, and both at ASD levels. These will then be compared with several other analyses. First, the end mean loss value for the normal run will be used to do a t-test with the end loss values for the perturbed networks. The end mean loss of the normal run is expected to be statistically lower than that of the other runs. Next, a similar test will be done with the starting mean loss values to judge whether there is a statistical difference in the network initialization. A percentage decrease will be done from the beginning value to the end value to determine how much each network improves. Finally, linear and exponential curves will be fitted to the values to determine which is a better fit for the data, and then the rate of decrease from the four runs will be compared. The normal model is expected to decrease mean loss at a faster rate, indicating more efficient learning.

Results

All model runs were conducted with an image vector size of 900 and 100 training sessions. The mean loss values for the four runs are pictured below.

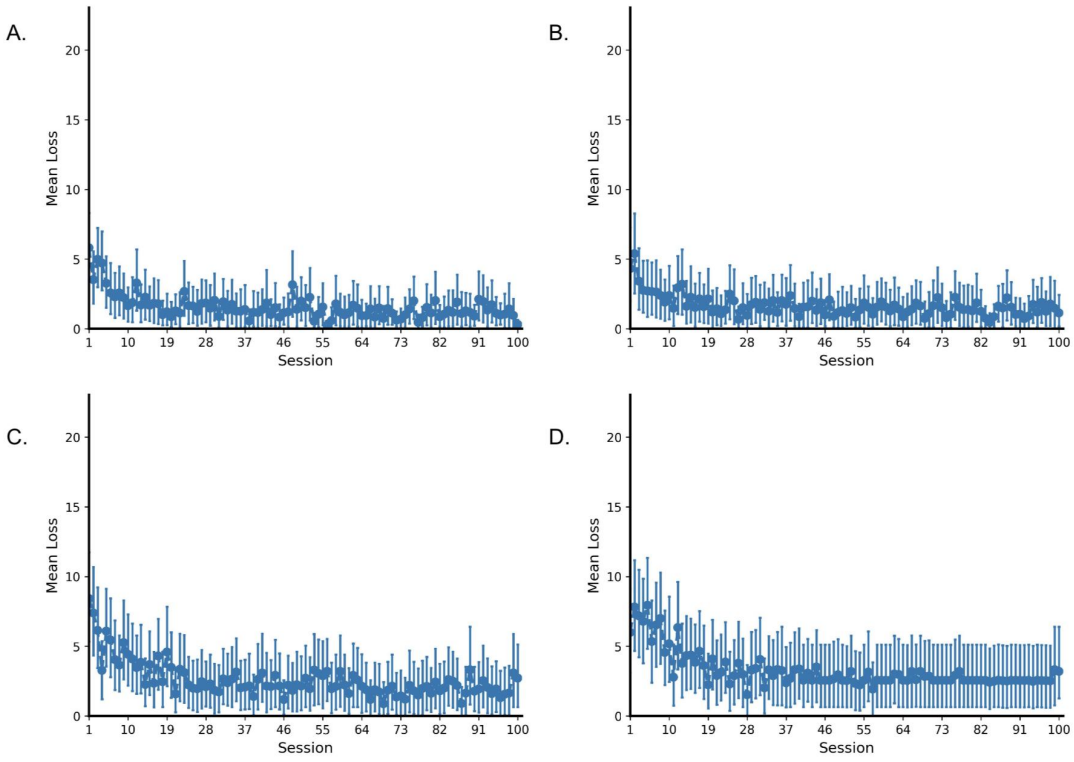

Figure 1. Mean Loss Values v. Session; A: CCL5 and Wnt Normal, B: CCL5 ASD and Wnt Normal, C: CCL5 Normal and Wnt ASD, D: CCL5 and Wnt ASD

Each dot indicates a session, with error bars defining a 95% confidence interval calculated from bootstrapping. All four models show a downward trend in loss, as expected of a neural network classifying images with more precision as it learns. There are observations that can be made from just the graphs. Both A and B, with Wnt at control levels, start from a lower mean loss than C and D, where Wnt was increased. This indicates the redundancy created by the addition of more nodes in sequential layers causes the model to have more loss at first. The control graph seems to have more variability compared to the three other graphs, while D, where both Wnt and CCL5 are changed, looks to be more stable. However, the confidence intervals for D are larger compared to the other three, indicating more variability within each training session. This could make sense because this test has both variables altered, whereas the rest have one or zero altered.

Initial and End Mean Loss Comparison

A 2-sample t test was done to compare both the initial and final mean losses of the normal run to the initial and final mean losses of the three perturbed runs. The test is one-tailed to measure if the control mean is statistically smaller than the means of the perturbed network. An asterisk indicates the value is statistically significant based on the alpha level of 0.10. A double asterisk indicates the value is statistically significant based on the alpha level of 0.05. All population sizes are n = 36, fulfilling the central limit theorem.

Table 1: Initial Mean Loss

	Mean	Sample SD	Test Statistic	P-value	df
Normal	5.8081	7.5692	-	-	-
CCL5 ASD/Wnt Normal	4.3203	8.0955	-0.8055	0.79	69.6861
CCL5 Normal/Wnt ASD	8.4235	9.7931	1.2678	0.10	65.8189
Both ASD	5.9964	9.4816	0.0931	0.46	66.7254

Table 2: Final Mean Loss

	Mean	Sample SD	Test Statistic	P-value	df
Normal	0.3115	0.9696	-	-	-
CCL5 ASD/Wnt Normal	1.1399	3.6863	1.3005	0.10*	39.8198
CCL5 Normal/Wnt ASD	2.7165	7.1671	1.9952	0.03**	36.2807
Both ASD	3.1980	8.0760	2.1292	0.02**	36.0088

The significant values show that the final mean loss in the perturbed networks is statistically greater than the mean loss in the control. However, there are no significant values for the initial mean loss. This result could indicate that the initial values do not statistically differ from each other, but the final values show that the perturbed networks do have an effect on the decrease in loss.

The percentage decrease from the initial mean loss to the final mean loss is also used as another measure to show how much each network learned and improved. For the control, the mean loss decreases by 94.64%, the CCL5 ASD/Wnt Normal decreases by 73.62%, the CCL5 Normal/Wnt ASD decreases by 67.75%, and Both ASD decreases by 46.67%. The network where the concentrations of the proteins were increased showed less improvement, specifically the network where both were changed, which showed the least improvement.

Regression Curves and Rate of Decrease in Loss

Regression was done for each of the mean loss graphs in order to find the best-fitting curve and then compare the decrease in the rate of loss for all four networks. Figures 2–5 show these graphs.

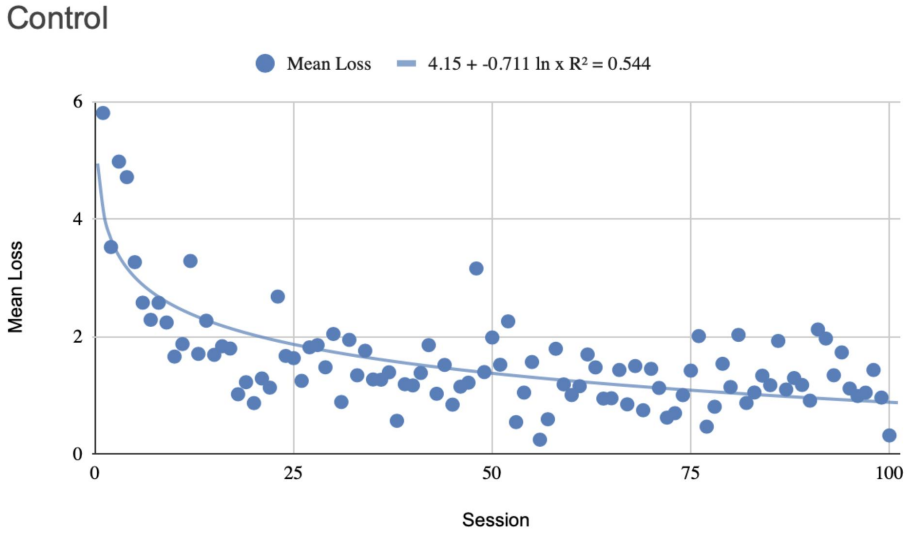

Figure 2. Control network. The regression curve with the highest R^2 value, a logarithmic curve, is displayed and plotted.

The equation for this curve is $\widehat{y} = 4.15 - 0.711ln(x)$ with an R^2 of 0.544 indicating a fairly strong correlation.

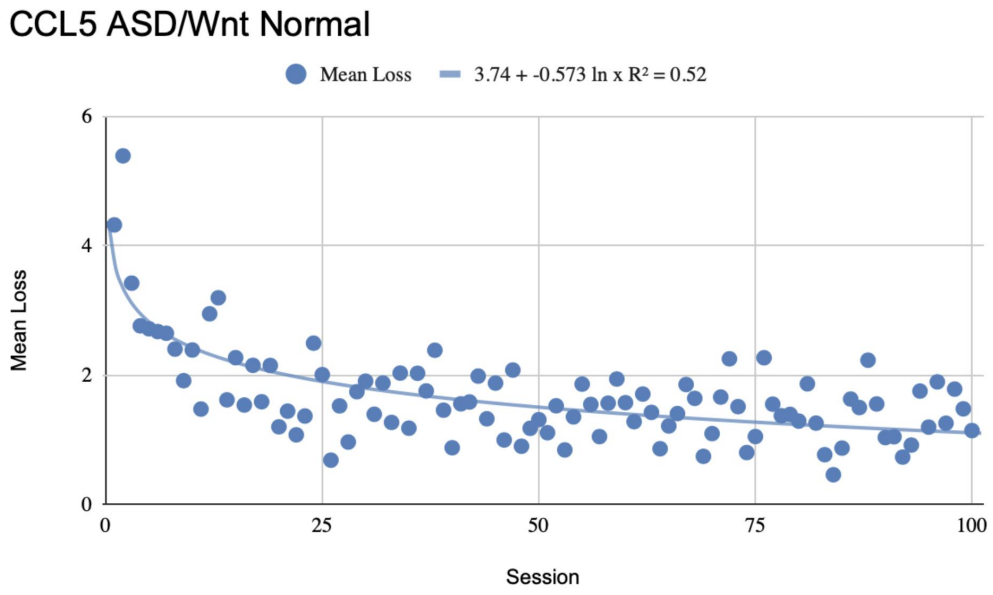

Figure 3. CCL5 ASD/Wnt Normal network. The regression curve with the highest R^2 value, a logarithmic curve, is displayed and plotted.

The equation for this curve is $\widehat{y} = 3.74 - 0.573ln(x)$ with an R^2 of 0.52 once again indicating a fairly strong correlation.

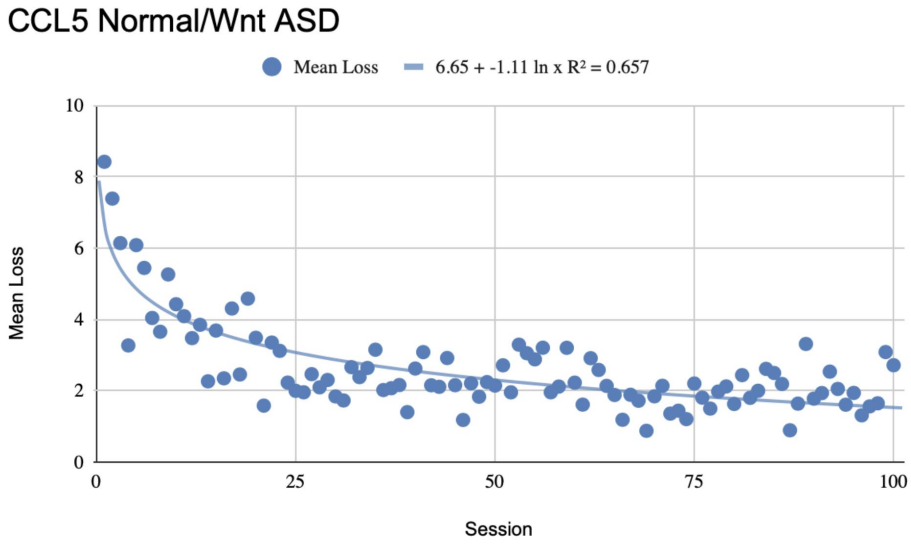

Figure 4. CCL5 Normal/Wnt ASD network. The regression curve with the highest R^2 value, a logarithmic curve, is displayed and plotted.

The equation for this curve is $\widehat{y} = 6.65 - 1.11ln(x)$ with an R^2 of 0.657 indicating a strong correlation.

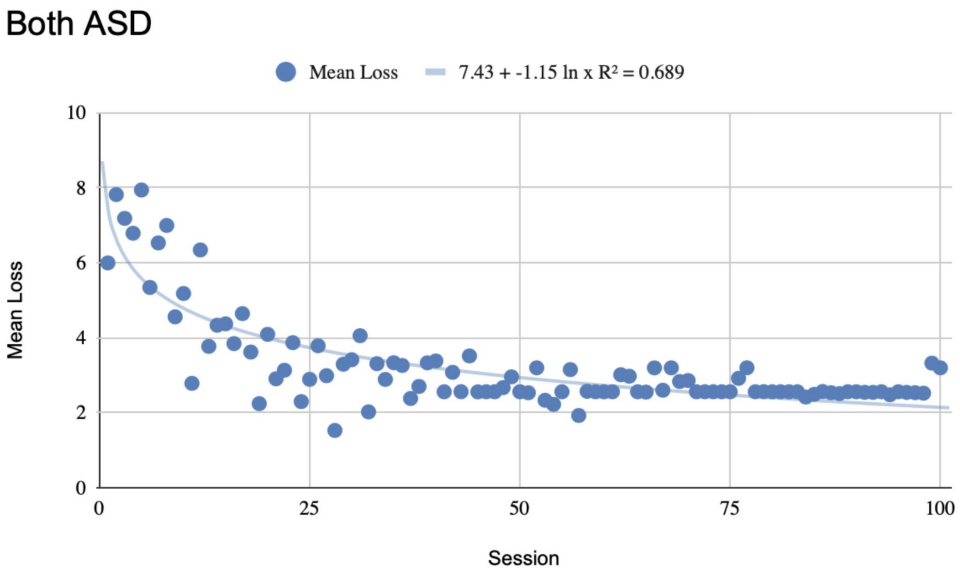

Figure 5. Both ASD values network. The regression curve with the highest R^2 value, a logarithmic curve, is displayed and plotted.

The equation for this curve is $\widehat{y} = 7.43 - 1.15ln(x)$ with an R^2 of 0.689 again indicating a strong correlation.

Logarithmic decay was the most accurate curve to fit for this data due to having the highest R^2 compared to other potential curve fits. The coefficients of the ln(x) term in these equations can be compared to signify how fast the loss decreases. With a smaller number, the loss decreases faster compared to a larger coefficient. For these equations, both the networks with the perturbed Wnt concentration have a smaller ln(x) coefficient than the two without the perturbed Wnt. However, the values are not too far apart, and the R2 values indicate that the unperturbed Wnt equations have more variability, which plays a role in the difference in coefficients.

Discussion

Several conclusions can be drawn from the results. First and most importantly, there is a defined statistical difference in how well this neural network will classify images with increases in Wnt and mTOR-activated CCL5 concentration. The networks fail to divide the images into their appropriate groups more often when their framework has been changed due to the creation of more connections and nodes. This reflects the true neurobiology, where increased CCL5 causes glutamatergic release while excess Wnt proteins help stabilize and allow for new synapses. The control network, compared to the three perturbed networks, was able to reach a low level of loss and had the greatest relative decrease.

However, the rate of decrease in loss of the control model was not found to be significantly larger than that of the other networks and, in fact, was slightly lower. This could be explained by the fact that there was an increased amount of variability in the control graph, as seen by the coefficient of determination. For example, three out of the first four data points in the control graph are underestimated by the fitted equation. Because the decay in logarithmic functions is fastest at lower numbers, the curve of best fit is underrepresenting that initial dramatic decay. But overall, the results of this study use more novel computation techniques to model the framework of autism spectrum disorders, specifically the effect of two perturbed pathways on visual processing, to show larger-scale representations of ASD impact.

Limitations

The main limitation regarding this project is the computing power needed to run neural networks with larger layers and more images. The training sessions were limited to 100 and the layer size to 900 nodes for this project. Adding more images causes long run times that do not show many

differences between the session count and layer size. With more powerful and efficient computers, changes can be made to more closely reflect the human brain.

The model also returns the accuracy of the testing phase. This project mainly focused on the loss during the training to reflect the learning that occurs in ASD, but the accuracy was found to be similar in all four networks. This was most likely due to the image classes being very distinct and the images themselves having a clearly defined focus. More images in this way could be used to better test the accuracy.

As a computational model, the results here can only predict and explain certain mechanisms that are part of ASD. It cannot take into account environmental factors such as behavioral therapy or specialized education that can augment the learning of a child with ASD. There is the ability to add more factors and account for environmental changes, but that is beyond the scope of this study.

Future Research

This project provides a model that is one of the first to incorporate neural networks into ASD modeling. Most research on this topic has been on the cellular or regional level, but using a neural network allows for a larger scale of connectivity, much more similar to that of the brain. ASD or other neurological disorders can be studied in this way because much of the brain works through signaling pathways and long connections. There is also the ability to quantify the effects of molecules important in these pathways, including Wnt and CCL5, as explored here. Wnt and CCL5 combined in this project created emergent properties that were not seen with either on their own. This type of research can be done with other molecules and signaling pathways that engage in crosstalk, like the Wnt and mTOR pathways.

Conclusion

In creating this model, we aimed to reflect two of the many mechanisms that are intertwined in ASD. The Wnt proteins that are used in signaling of the Wnt pathway and CCL5 activated by the mTOR pathway are found in excess concentrations in children with ASD. CCL5 excess causes the excitotoxicity of glutamate, which plays a key role in plasticity. Elevated Wnt protein levels allow for more synaptic stability and block the pruning of unnecessary synapses. Accurately modeling defects in large-scale connections in the brain is tricky to do biologically, and using a neural network can capture similar behavior without risk.

The results show a statistically lower loss of image accuracy for the control compared to all three test runs. This is crucial because it shows that a neural network model can represent aspects of ASD in terms of long-range neuron communication. The effects of these two proteins are important to gain a deeper understanding of ASD mechanisms and are applicable to other pathways implicated in this disorder. However, there does not seem to be a conclusive difference in learning rates for each tested network compared to the model, which could be due to the limited number of training sessions, layer sizes, and images. By empirically showing that the model can accurately reflect the signaling in ASD, Wnt and CCL5 are shown to be major players in the system. It also provides a model that relies on population dynamics, which can be used to learn about and treat ASD network activity.

References

1. P. Ashwood, P. Krakowiak, I.Hertz-Picciotto, R. Hansen, I.N. Pessah, J. Van de Water. Associations of impaired behaviors with elevated plasma chemokines in autism spectrum disorders. *J Neuroimmunol.* **232**, 196-199 (2011).

2. M.D. Thye, H.M. Bednarz, A.J. Herringshaw, E.B. Sartin, R.K. Kana. The impact of atypical sensory processing on social impairments in autism spectrum disorder. *Dev Cogn Neurosci.* **29**, 151-167 (2018).
3. Y.M.Y. Han, S.Y. Yau, M.M.Y. Chan, C.K. Wong, A.S. Chan. Altered Cytokine and BDNF Levels in Individuals with Autism Spectrum Disorders. *Brain Sci.* **12**, 460 (2022).
4. M. Sahin, M. Sur. Genes, circuits, and precision therapies for autism and related neurodevelopmental disorders. *Science.* **350**, 6263 (2015).
5. S. Kumar, K. Reynolds, Y. Ji, R. Gu, S. Rai, C.J. Zhou. Impaired neurodevelopmental pathways in autism spectrum disorder: a review of signaling mechanisms and crosstalk. *J Neurodev Disord.* **11**, 1-10 (2019).
6. V. Musante, F. Longordo, E. Neri, M. Pedrazzi, F. Kalfas, P. Severi, M. Raiteri, A. Pittaluga. RANTES modulates the release of glutamate in human neocortex. *J Neurosci*. **28**, 12231-12240 (2008).
7. S. Di Prisco, M. Summa, V. Chellakudam, P.I. Rossi, A. Pittaluga RANTES-mediated control of excitatory amino acid release in mouse spinal cord. *J Neurochem*. **121**, 428-437 (2012).
8. M.F. Lanfranco, I. Mocchetti, M.P. Burns, S. Villapol. Glial- and Neuronal-Specific Expression of CCL5 mRNA in the Rat Brain. *Front Neuroanat.* **11**, 137 (2018).
9. A.B. Patel, I. Tsilioni, S.E. Leeman, T.C. Theoharides. Neurotensin stimulates sortilin and mTOR in human microglia inhibitable by methoxyluteolin, a potential therapeutic target for autism. *Proc Natl Acad Sci U S A.* **113**, E7049-E7058 (2016).
10. B. Wang, Y. Qin, Q. Wu, X. Li, D. Xie, Z. Zhao, S. Duan. mTOR Signaling Pathway Regulates the Release of Proinflammatory Molecule CCL5 Implicated in the Pathogenesis of Autism Spectrum Disorder. *Front Immunol*. **13**, 818518 (2022).

11. A. Pittaluga. CCL5-Glutamate Cross-Talk in Astrocyte-Neuron Communication in Multiple Sclerosis. *Front Immunol.* **8**, 1079 (2017).
12. P.M. Martin, X. Yang, N. Robin, E. Lam, J.S. Rabinowitz, C.A. Erdman, J. Quinn, L.A. Weiss, S.P. Hamilton, P.Y. Kwok, R.T Moon, B.N Cheyette. A rare WNT1 missense variant overrepresented in ASD leads to increased Wnt signal pathway activation. *Transl Psychiatry.* **3**, e301 (2013).
13. V.H. Gazestani, T. Pramparo, S. Nalabolu, B.P. Kellman, S. Murray, L. Lopez, K. Pierce, E. Courchesne, N.E. Lewis. A perturbed gene network containing PI3K-AKT, RAS-ERK and WNT-β-catenin pathways in leukocytes is linked to ASD genetics and symptom severity. *Nat Neurosci.* **22**, 1624-1634 (2019).
14. S. Teo, P.C. Salinas. Wnt-Frizzled Signaling Regulates Activity-Mediated Synapse Formation. *Front Mol Neurosci.* **14**, 683035 (2021).
15. A. Patapoutian, L.F. Reichardt. Roles of Wnt proteins in neural development and maintenance. *Curr Opin Neurobiol.* **10**, 392-399 (2000).
16. C. Bonansco, W. Cerpa, N.C. Inestrosa. How Are Synapses Born? A Functional and Molecular View of the Role of the Wnt Signaling Pathway. *Int J Mol Sci.* **24**, 708 (2022).
17. S.B. Rosso, N.C. Inestrosa. WNT signaling in neuronal maturation and synaptogenesis. *Front Cell Neurosci.* **7**, 103 (2013).
18. L. Cuitino, J.A. Godoy, G.G. Farías, A. Couve, C. Bonansco, M. Fuenzalida, N.C. Inestrosa. Wnt-5a modulates recycling of functional GABAA receptors on hippocampal neurons. *J Neurosci.* **30**, 8411-8420 (2010).
19. A. Khaleghi, H. Zarafshan, S.R. Vand, M.R. Mohammadi. Effects of Non-invasive Neurostimulation on Autism Spectrum Disorder: A Systematic Review. *Clin Psychopharmacol Neurosci.* **18**, 527-552 (2020).

20. A.A. Anashkina, E.I. Erlykina. Molecular Mechanisms of Aberrant Neuroplasticity in Autism Spectrum Disorders (Review). *Sovrem Tekhnologii Med.* **13**, 78-91 (2021).

21. B. Ataman, J. Ashley, M. Gorczyca, P. Ramachandran, W. Fouquet, S.J. Sigrist, V. Budnik. Rapid activity-dependent modifications in synaptic structure and function require bidirectional Wnt signaling. *Neuron.* **57**, 705-718 (2008).

22. V. Budnik, P.C. Salinas. Wnt signaling during synaptic development and plasticity. *Curr Opin Neurobiol.* **21**, 151-159 (2011).

23. F. McLeod, P.C. Salinas. Wnt proteins as modulators of synaptic plasticity. *Curr Opin Neurobiol.* **53**, 90-95 (2018).

24. G. Tang, K. Gudsnuk, S.H. Kuo, M.L. Cotrina, G. Rosoklija, A. Sosunov, M.S. Sonders, E. Kanter, C. Castagna, A. Yamamoto, Z. Yue, O. Arancio, B.S. Peterson, F. Champagne, A.J. Dwork, J. Goldman, D. Sulzer. Loss of mTOR-dependent macroautophagy causes autistic-like synaptic pruning deficits. *Neuron.* **83**, 1131-1143 (2014).

25. M.L. Chow, T. Pramparo, M.E. Winn, C.C. Barnes, H.R. Li, L. Weiss, J.B. Fan, S. Murray, C. April, H. Belinson, X.D. Fu, A. Wynshaw-Boris, N.J. Schork, E. Courchesne. Age-dependent brain gene expression and copy number anomalies in autism suggest distinct pathological processes at young versus mature ages. *PLoS Genet.* **8**, e1002592 (2012).

26. Y.M. Han, W.K. Cheung, C.K. Wong, S.L. Sze, T.W. Cheng, M.K. Yeung, A.S. Chan. Distinct Cytokine and Chemokine Profiles in Autism Spectrum Disorders. *Front Immunol.* **8**, 11 (2017).